Ultra-High Selectivity Pulsed Plasmachemical Deposition Reaction Pathways

Andrea Carletto and Jas Pal S. Badyal*

Chemistry Department, Science Laboratories, Durham University, Durham DH1 3LE, England, UK

* Corresponding author email: j.p.badyal@durham.ac.uk

CONTENTS

TABLE OF CONTENTS ENTRY

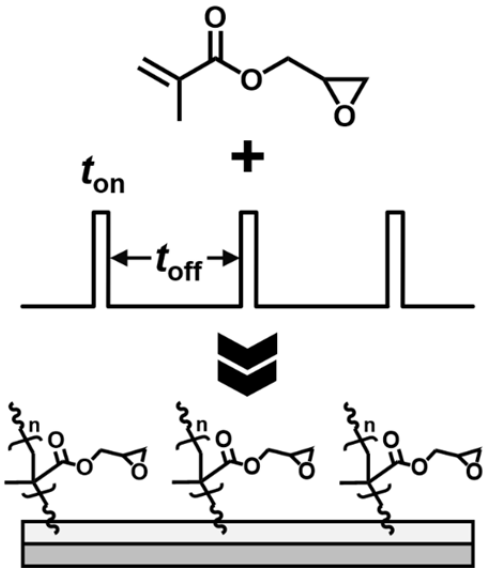

High selectivity chemical reaction pathways can be attained by using low duty cycle pulsed electrical discharges.

ABSTRACT

Glycidyl methacrylate pulsed plasmas have been investigated using time-resolved in situ mass spectrometry. At low pulsed plasma duty cycles, monomer fragmentation leading to the formation of polymerisation initiator species occurs within each short electrical discharge pulse (t_{on} = microseconds timescale). This is followed by conventional step-wise monomer addition polymerisation occurring during the subsequent extended off-period (t_{off} = milliseconds timescale), culminating in the growth of well-defined poly(glycidyl methacrylate) chains. Key attributes associated with this high selectivity pulsed plasmachemical functional thin film synthesis approach are absence for the requirement of any additional chemicals (catalyst, solvent, etc.) in combination with very low power consumption (mW) and ambient temperature.

INTRODUCTION

High selectivity chemical reaction pathways are of fundamental importance in modern chemistry and have in the past been attained via a variety of conventional approaches, including catalysis (heterogeneous, homogeneous, enzymes), high pressure kinetic methods, mixing techniques, and solvent effects.[1,2,3,4,5,6,7] Although these have proven to be selective towards the formation of specific chemical products, there can be inherent limiting factors. For instance, in the case of catalytic processes where metals are often employed, such systems can be expensive and seldom reusable; whilst high pressure, mixing, and solvent-based syntheses can be environmentally unfriendly as well as involving multiple steps.[8,9,10,11]

Non-equilibrium (low temperature) electrical discharges offer the potential for single-step and low cost chemical syntheses. However, the main drawback has been poor chemical selectivity.[12] Pulsing such plasmas potentially provides means to control the lifetimes of reactive intermediate species, and thereby enable control over reaction pathways. In the case of pulsed plasma excitation of organic monomers, through a careful selection of electrical discharge parameters, it is possible to achieve high levels of molecular control for the deposited film composition and its properties.[13,14] For example, hundreds of millions of smartphones have been protected against water damage using such functional nanocoatings.[15] By using a variety of surface characterisation techniques (including ToF-SIMS, MALDI-MS, XPS, FTIR), strong structural similarities have been found with analogous conventional wet chemical synthesis step-growth polymers.[16,17,18]

However, the underlying mechanism for the growth of such structurally well-defined pulsed plasma functional films is poorly understood. Previous in situ mass spectrometry studies of polymerising plasmas have identified oligomer formation, but an absence of ultra-high selectivity reaction pathways.[19,20,21,22,23,24,25,26] Time-resolved in situ mass spectrometry studies of pulsed electrical discharges, offer the scope for probing plasmachemical reaction pathways during the respective on- and off-time windows (t_{on} and t_{off}). In this study, glycidyl methacrylate precursor is investigated following earlier reports of the pulsed plasma deposition of structurally well-defined poly(glycidyl methacrylate) films (as confirmed by XPS and ToF-SIMS), Structure 1.[16,27] Furthermore, glycidyl methacrylate contains two reactive

functionalities (acrylate carbon–carbon double bond and epoxide group)—the selective plasmachemical activation of one of these groups (acrylate) highlights the versatility of pulsed plasma deposition as a method for surface functionalisation. Such epoxide-functionalized surfaces are sought for technological applications such as, chemosensors, biosensors, drug delivery, biomolecule arrays, electroless metal deposition, and anti-biofouling surfaces.[28,29,30,31,32,33,34,35]

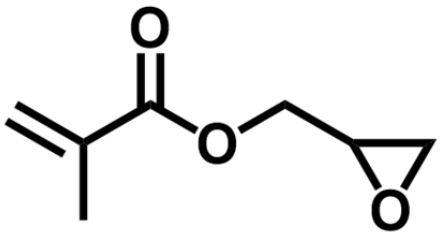

Structure 1: Glycidyl methacrylate

EXPERIMENTAL

Time-resolved in situ mass spectrometry measurements were made during pulsed plasma excitation of glycidyl methacrylate precursor (+97%, Sigma Aldrich Co.), Figure 1. A cylindrical glass reactor (volume 2,943 cm^3), was pumped down to a base pressure of 8 $\times 10^{-3}$ mbar, via a liquid nitrogen cold trap attached to a turbomolecular drag pump (model TPD 022, Pfeiffer Vacuum Technology AG) which was backed by a diaphragm pump (model N813.4 ANE, KNF Neuberger GmbH). A copper coil (7 mm diameter, 4 turns, spanning 10.5 cm) wrapped around the glass chamber was connected to a 13.56 MHz radio frequency (RF) power supply (model RFG 600SE, Coaxial Power Systems Ltd.) in combination with a L–C circuit matching network (to minimise reflected power). A pulse signal generator (model TG503, Thurlby Thandar Instruments Ltd.) was used to trigger the RF power supply and monitored with an oscilloscope (model OX 530, Metrix Ltd.). Prior to each experiment, the chamber was cleaned by running a 50 W oxygen plasma (0.2 mbar pressure) until no contaminant species were detected by mass spectrometry. Glycidyl methacrylate precursor was loaded into a sealable glass tube, degassed via at least 5 freeze–pump–thaw cycles, and attached to the reactor. The monomer was then purged through the system at a pressure of 0.1 mbar via a fine control needle

valve (model 145-217-4P4PC, Meggitt Avionics Ltd.) for 20 min, followed by electrical discharge ignition. For pulsed plasmas, an on-period (t_{on}) of 30 μs and an off-period (t_{off}) of 10 ms were used in conjunction with 15 W of continuous wave power input during the on-period (P_{on}). These parameters were chosen on the basis of earlier optimisation studies reported for high structural retention of pulsed plasma deposited poly(glycidyl methacrylate) nanolayers.[16] After each experiment, the pulsed plasma poly(glycidyl methacrylate) nanolayer was oxidised off the chamber walls by running a 50 W oxygen plasma (0.2 mbar pressure) until no carbonaceous species were detected by mass spectrometry.

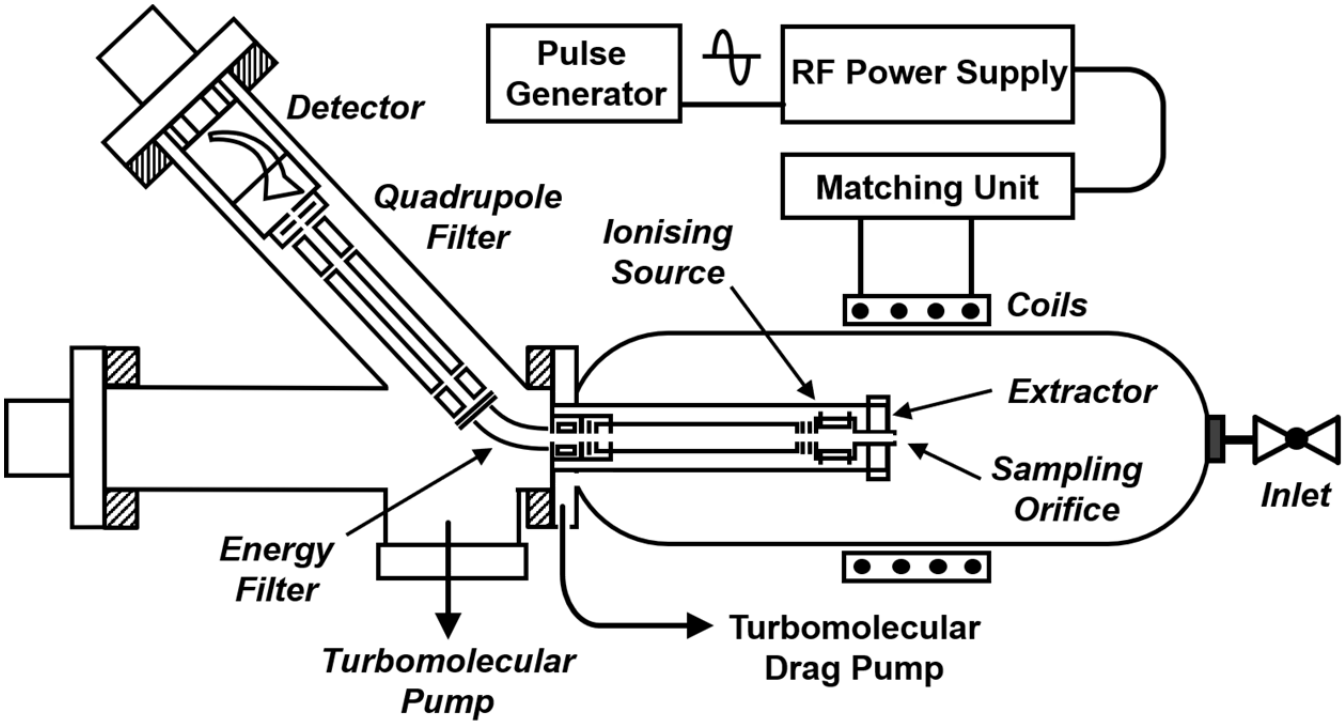

Figure 1: Experimental set-up for in situ mass spectrometry of pulsed plasmas.

An electrostatic quadrupole mass spectrometer probe (model HAL EQP 2500, Hiden Analytical Ltd.), with a 200 μm orifice was positioned inside the plasma chamber, Figure 1. The mass spectrometer analyser was pumped by a turbomolecular pump (model TMU 260, Pfeiffer Vacuum Technology AG) which was backed by a rotary vane pump (model DUO 2.5, Pfeiffer Vacuum Technology AG) to give a mass spectrometer base pressure of better than 2×10^{-9} mbar. The electron impact ionisation source of the mass spectrometer was operated at low energy (20 eV) in order to avoid excessive fragmentation during the detection of neutral and

radical plasma species. In addition, ionised gaseous species (plasma ions) were sampled directly from within the electrical discharge through the 200 μm radius end cap orifice by switching off the electron impact ionisation source. Mass spectrometer tuning was undertaken by following the standard procedure recommended by the instrument manufacturer. Low mass fragments had higher ion energies whilst high mass fragments had lower ion energies. Hence, appropriate ion energy tuning was chosen according to the mass range to be investigated.

For time-resolved pulsed plasma measurements, signal gating of the mass spectrometer detector enabled any specified time window (t_{on} or t_{off}) to be monitored, Figure 2. This was achieved by using an additional pulse signal generator (model TGP110, Thurlby Thandar Instruments Ltd.) connected to the mass spectrometer interface unit (MSIU) through a transistor-transistor logic (TTL) input. One pulse signal generator was employed to trigger both the plasma duty cycle ignition and the other pulse signal generator, where the latter then triggered the mass spectrometer ion counting detector either throughout the whole duty cycle or selectively during the t_{on} or t_{off} time windows.[36,37,38,39,40]

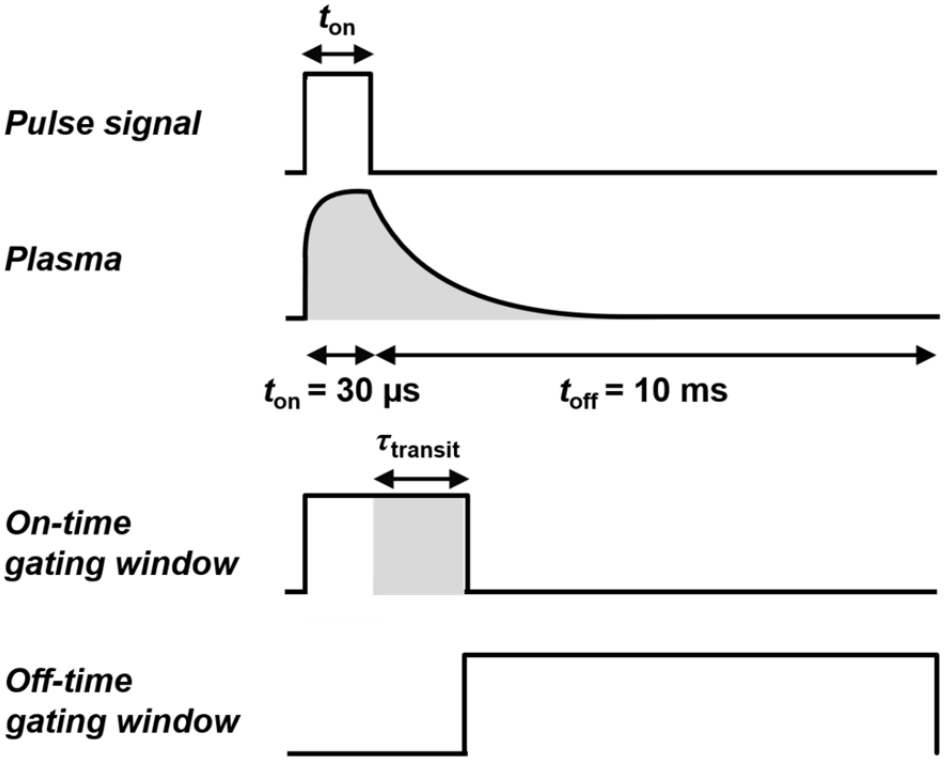

Figure 2: Time-resolved mass spectrometer pulsed plasma gating measurements.

For the time-resolved mode of analyser operation, the time taken for ions to transit the probe and reach the mass spectrometer detector is defined as the transit time ($\tau_{transit}$). This parameter is dependent upon the ion mass (m), the path length of the ion transit (s), and the electrical potential applied across the region (V), where $\tau_{transit}$ is given as being proportional to $s\sqrt{m/2eV}$.[41,42,43,44,45] The overall ion transit time can be calculated by summing the individual transit times for each region of the probe, namely the extractor, energy analyser, mass filter, and detector.[46,47,48] In order to measure up to a mass of 450 *m/z*, the mass spectrometer had a transit time, $\tau_{transit}$ = 300 µs. Therefore, the detector signal gating window was chosen to be 330 µs (corresponding to $t_{on} + \tau_{transit}$) for pulse on-period (t_{on}) measurements, whilst for pulse off-period (t_{off}) scans, this window was shifted to begin detecting 300 µs after t_{on}, and detection allowed to continue until the end of the pulse cycle, as illustrated in Figure 2.[45]

RESULTS

(a) Electron-Impact Glycidyl Methacrylate Precursor Fragmentation

Low energy (20 eV) electron-impact ionisation avoids extensive molecular fragmentation of glycidyl methacrylate precursor vapour, Figure 3. The main mass fragments formed are at 41, 43, 57, and 69 *m/z,* which correspond to specific bond cleavages within the molecule.[49,50,51,52] The parent molecular ion mass signal (142 *m/z*) and protonated molecular ion (143 *m/z*) were both absent.[53]

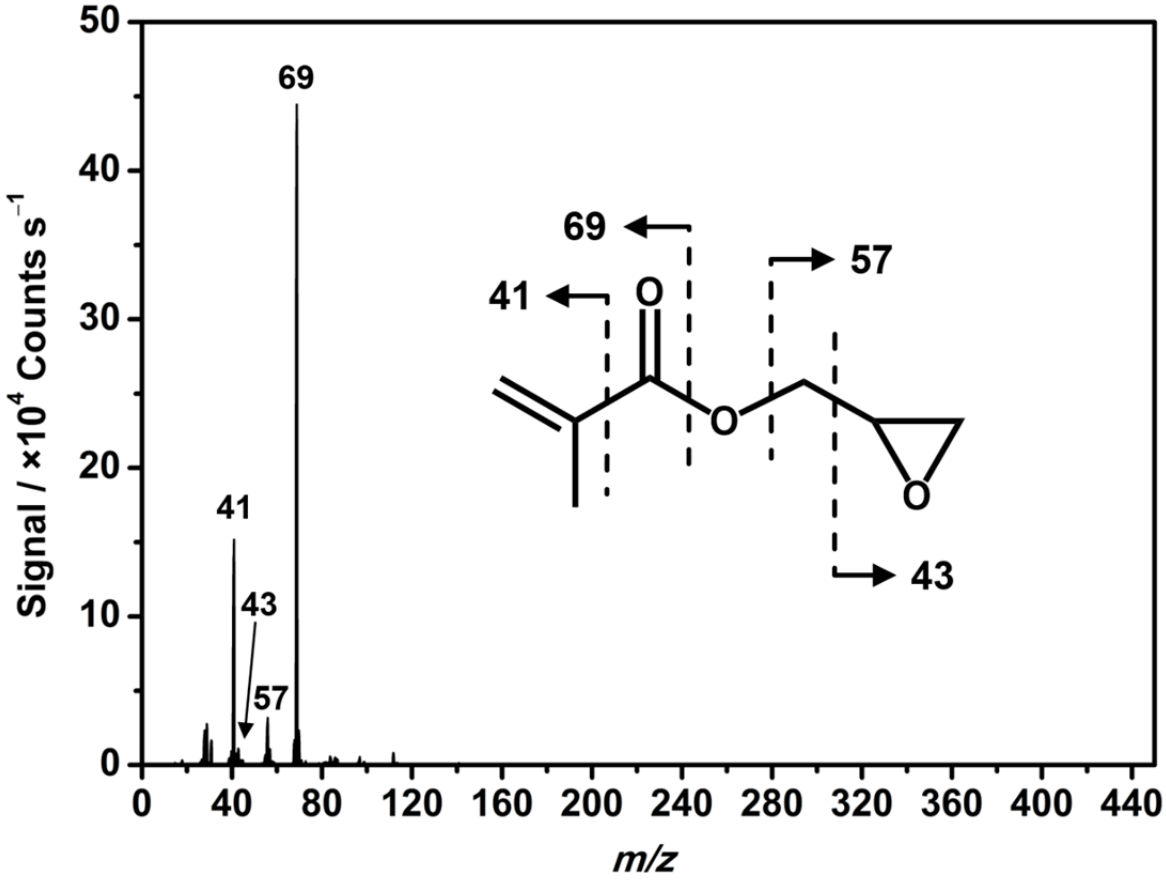

Figure 3: 20 eV electron-impact ionisation mass spectrum of glycidyl methacrylate monomer vapour, (0.1 mbar pressure). Mass spectrometer tuning optimised on 69 *m/z* mass signal.

(b) Positive Plasma Ion Species

In contrast to the absence of any parent molecular ion peak in the electron-impact ionisation mass spectrum of glycidyl methacrylate precursor (Figure 3), the protonated molecular ion peak (143 *m/z*) is present in the time-averaged positive ion mass spectrum of glycidyl methacrylate pulsed plasma, Figure 4. Moreover, the formation of new well-defined oligomer species at higher masses is evident corresponding to increasing integer number addition of glycidyl methacrylate monomer molecular mass repeat units (demonstrative of high selectivity). These arise as a consequence of step-wise glycidyl methacrylate monomer addition polymerisation from two initiator species—the main low energy electron impact fragmentation ion for glycidyl methacrylate monomer (69 *m/z*) and protonated glycidyl methacrylate precursor (143 *m/z*), Figure 3 and Figure 4, respectively.

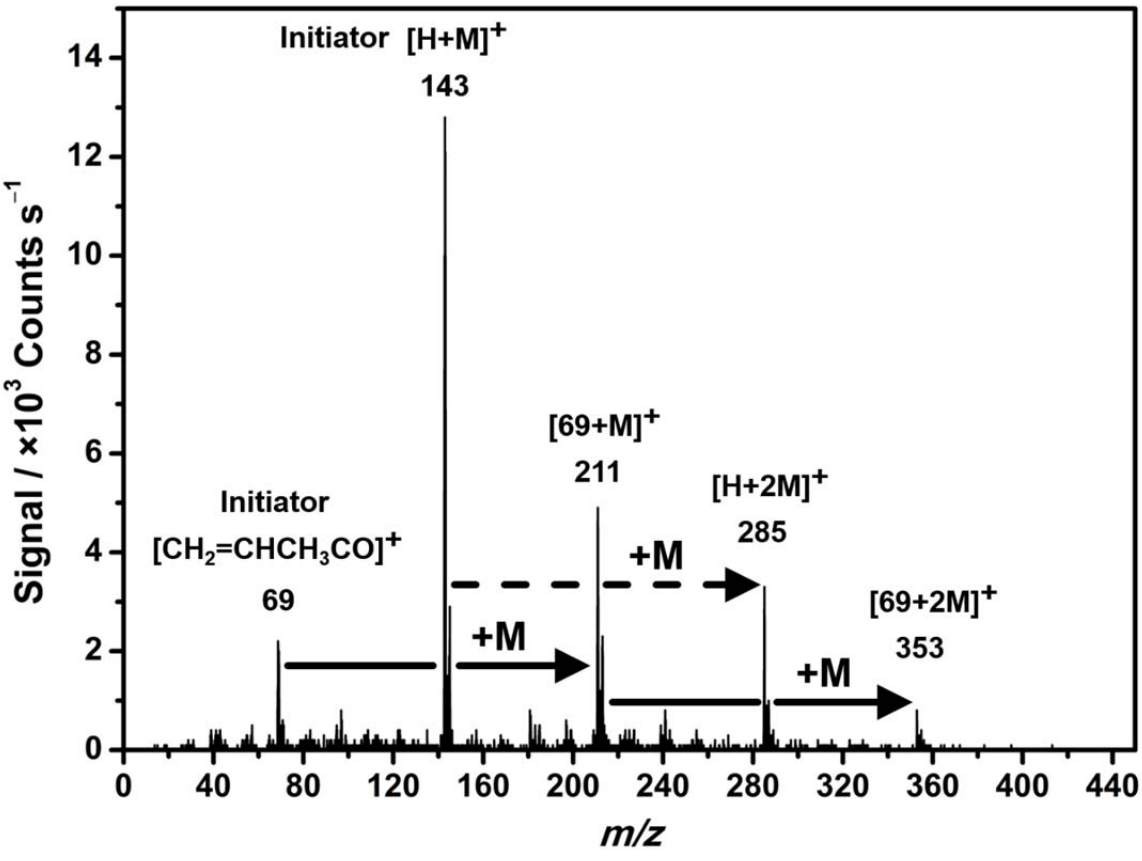

Figure 4: Time-averaged positive plasma ion mode mass spectrum of glycidyl methacrylate pulsed plasma (t_{on} = 30 µs, t_{off} = 10 ms, P_{on} = 15 W, and 0.1 mbar pressure). Mass spectrometer tuning optimised on 285 *m/z* mass signal.

Time-resolved mass spectrometry of glycidyl methacrylate pulsed plasmas detected the presence of a variety of positive ions during the electrical discharge on-period (t_{on}), Figure 5. These were low mass fragments (19, 28, 41, 43, 57, 69 and 143 m/z), with the main electron-impact molecular fragment (69 *m/z*) of glycidyl methacrylate monomer and the protonated precursor ion (143 *m/z*) being predominant within the on-period window, i.e. the formation of initiator species required for subsequent step-wise monomer addition polymerisation during the off-period, Figure 5.

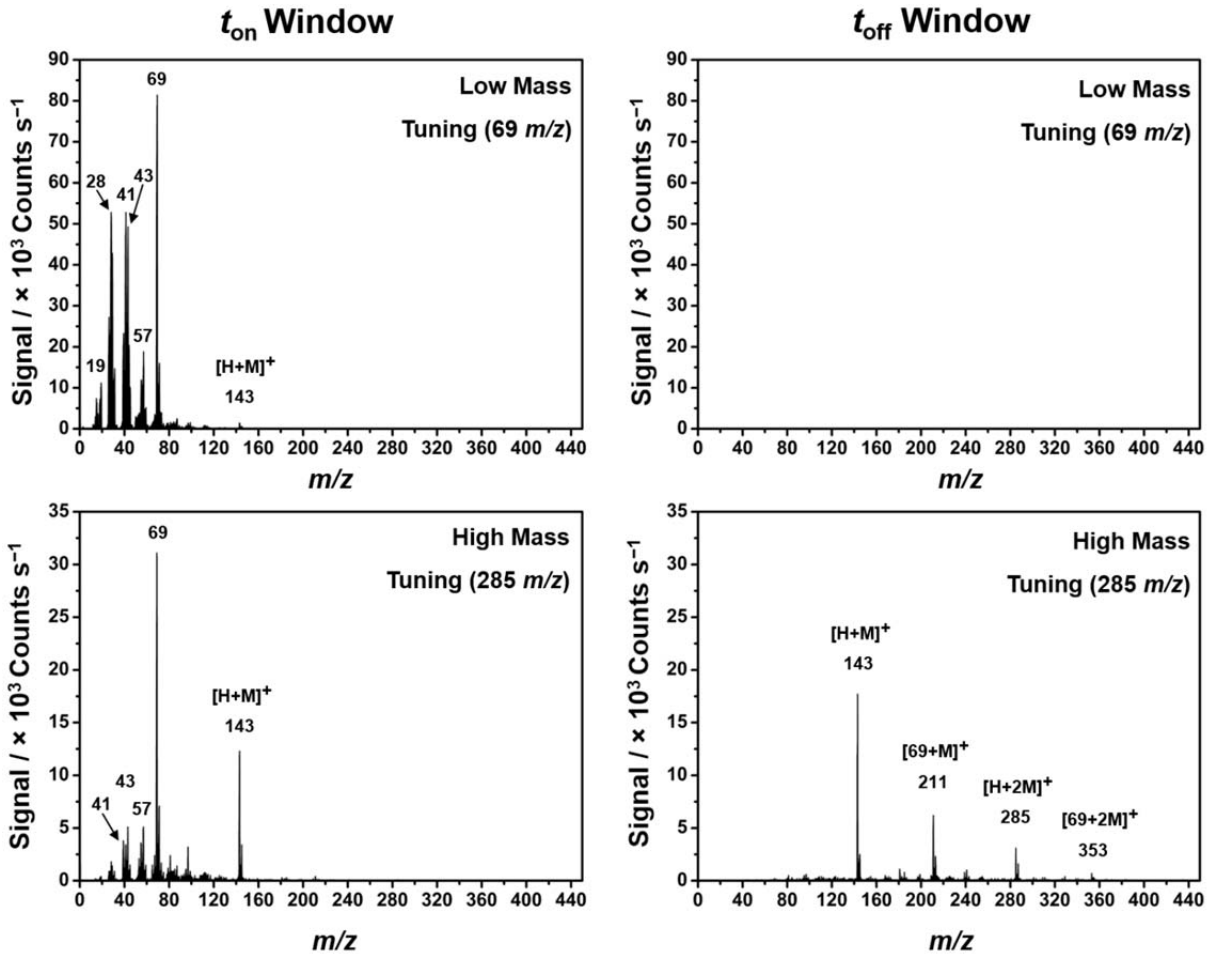

Figure 5: Low and high mass tuning time-resolved positive plasma ion mode mass spectra of glycidyl methacrylate pulsed plasma (t_{on} = 30 µs, t_{off} = 10 ms, P_{on} = 15 W, and 0.1 mbar pressure).

Monitoring of the subsequent off-period (t_{off}) window revealed exclusive (high selectivity) step-wise addition of glycidyl methacrylate monomer repeat units to both of the aforementioned on-period (t_{on}) window cation initiator species (69 and 143 *m/z*), leading to well-defined polymer chain growth over a time scale of about 5 ms—with longer (higher

mass) polymer chain ions becoming more prominent over time, Figure 6. Beyond this time frame of 5 ms, these polymer cations disappear due to recombination processes, film deposition, and decrease in ion energy (detuning of the mass spectrometer). Regardless, it is clear that the polymeric cations do indeed survive beyond the short on-period (t_{on} = 30 µs).

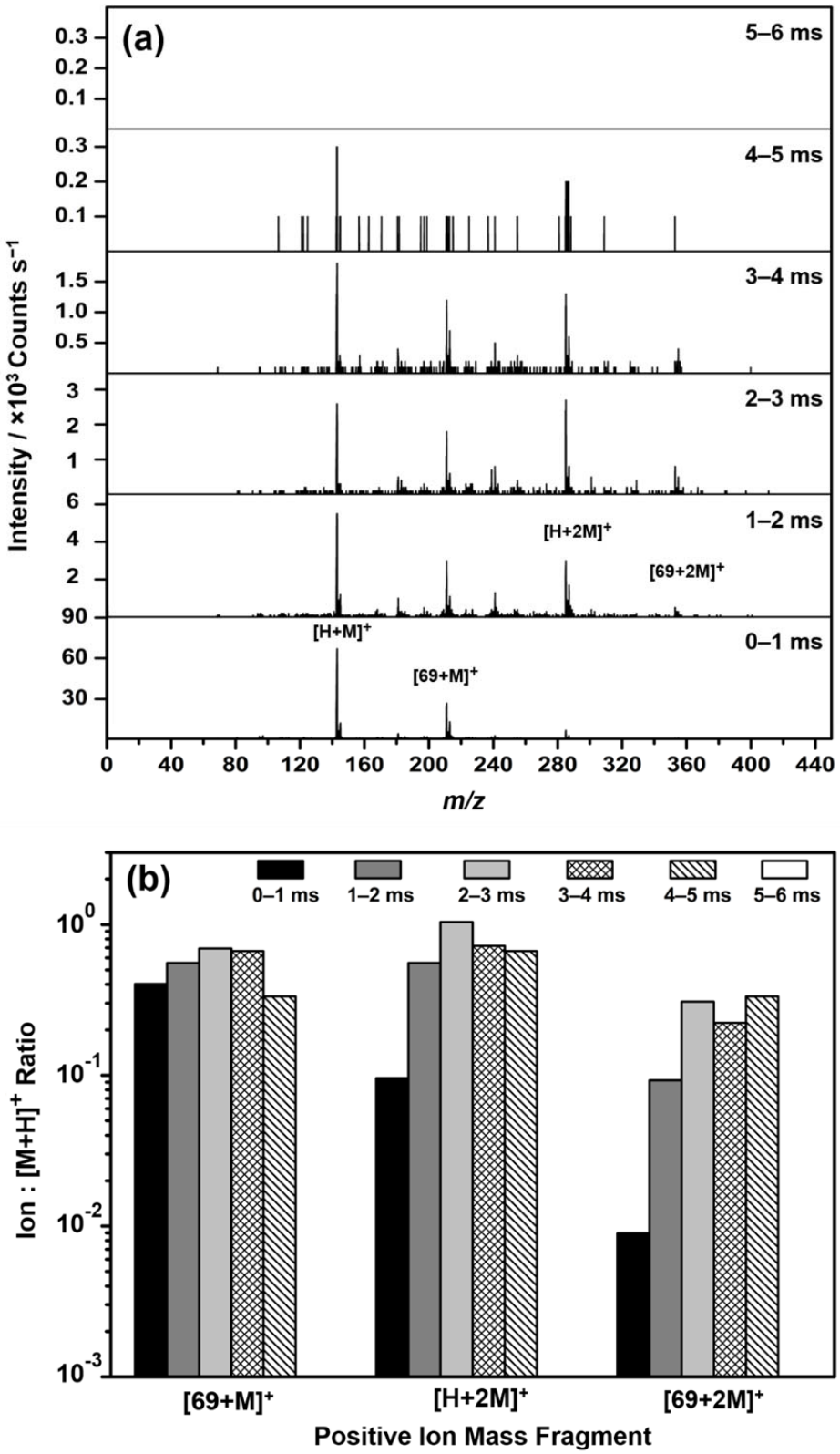

Figure 6: (a) Off-period positive ion mass mode spectra taken during consecutive 1 ms sampling time windows for glycidyl methacrylate pulsed plasma (t_{on} = 30 µs, ms t_{off} = 10 ms, P_{on} = 15 W, and 0.1 mbar pressure); and (b) variation of positive ion mass mode fragments between consecutive 1 ms sampling time windows during the off-period, showing relative positive ion : protonated molecular ion (143 *m/z*) intensity ratios. Note the complete disappearance of positive ion species after 5 ms. Mass spectrometer tuning optimised on 285 *m/z* mass signal.

(c) Neutral Plasma Species

Low energy (20 eV) electron-impact ionisation mass spectrometry of neutral pulsed plasma species (including radicals) detected similar fragments to those observed during positive plasma ion sampling, with the main glycidyl methacrylate electron-impact fragment being 69 *m/z*, Figure 3 and Figure 7. This species in combination with hydrogen atom addition to monomer (143 *m/z*) act as radical initiators for step-wise monomer addition polymerisation.

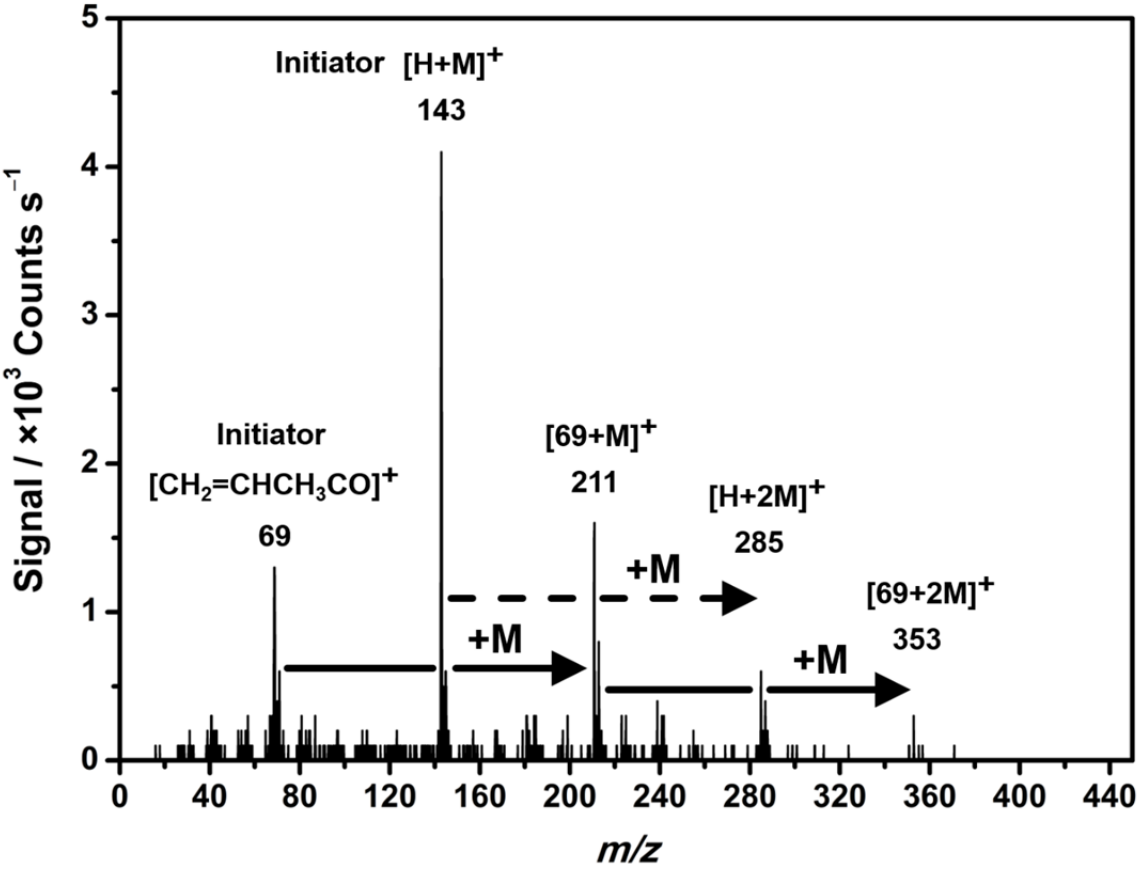

Figure 7: Time-averaged 20 eV electron-impact ionisation mass spectrum of glycidyl methacrylate pulsed plasma (t_{on} = 30 µs, t_{off} = 10 ms, P_{on} = 15 W, and 0.1 mbar pressure). Mass spectrometer tuning optimised on 211 *m/z* mass signal.

As observed previously during positive plasma ion mass spectrometer detection mode, 69 *m/z* and 143 *m/z* initiator species are created during the short pulsed plasma time-on (t_{on}) window, Figure 8. Polymer chain growth occurs within the extended pulsed plasma off-period (t_{off}) window, with longer growing (higher mass) chain signal intensities rising over time, Figure 9. The drop in overall intensity can be attributed to recombination processes as well as film deposition.

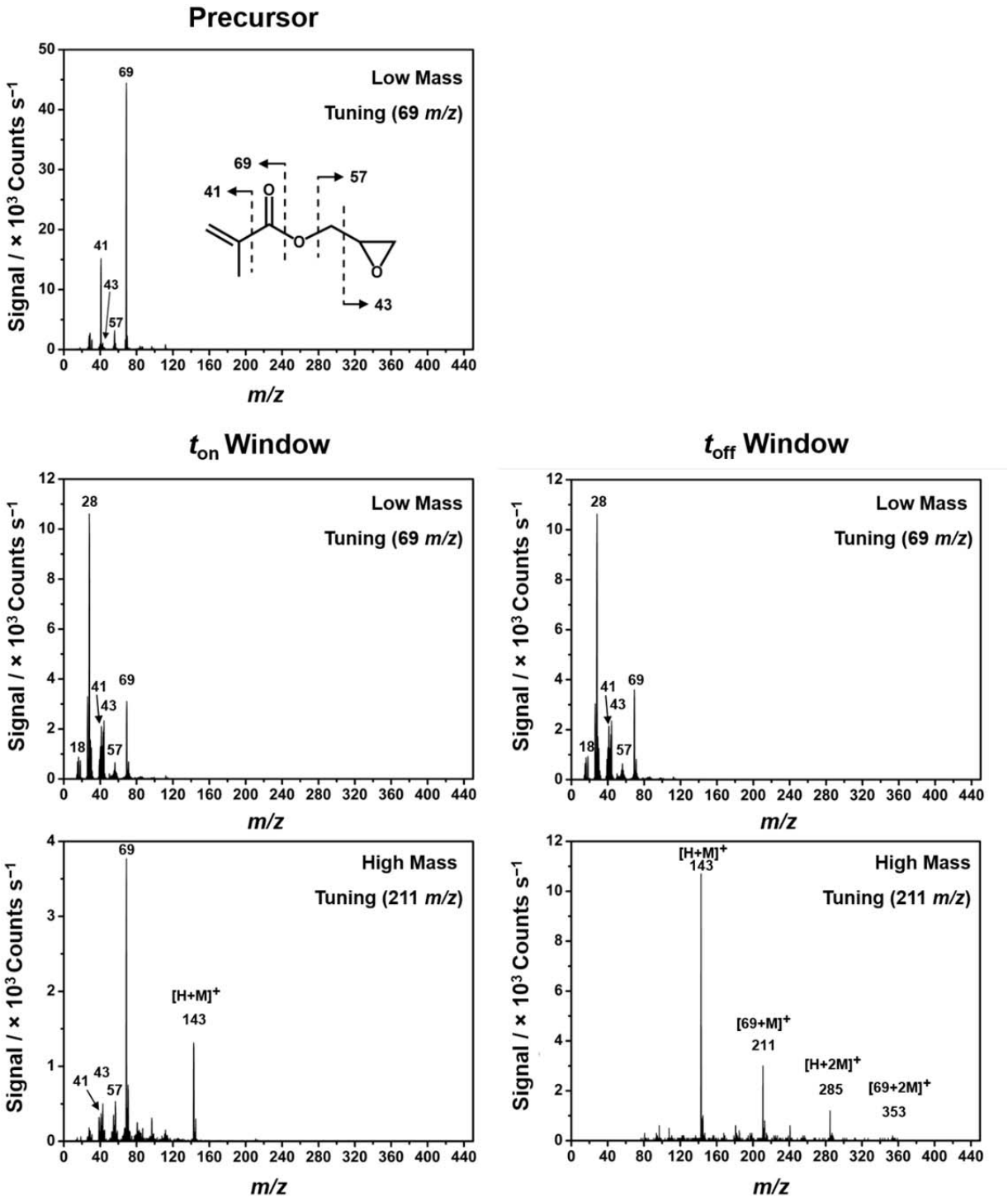

Figure 8: Low and high mass tuning time-resolved 20 eV electron-impact ionisation mass spectra of glycidyl methacrylate monomer vapour (top left) and pulsed plasma (middle and bottom spectra, with t_{on} = 30 µs, t_{off} = 10 ms, P_{on} = 15 W, and 0.1 mbar pressure).

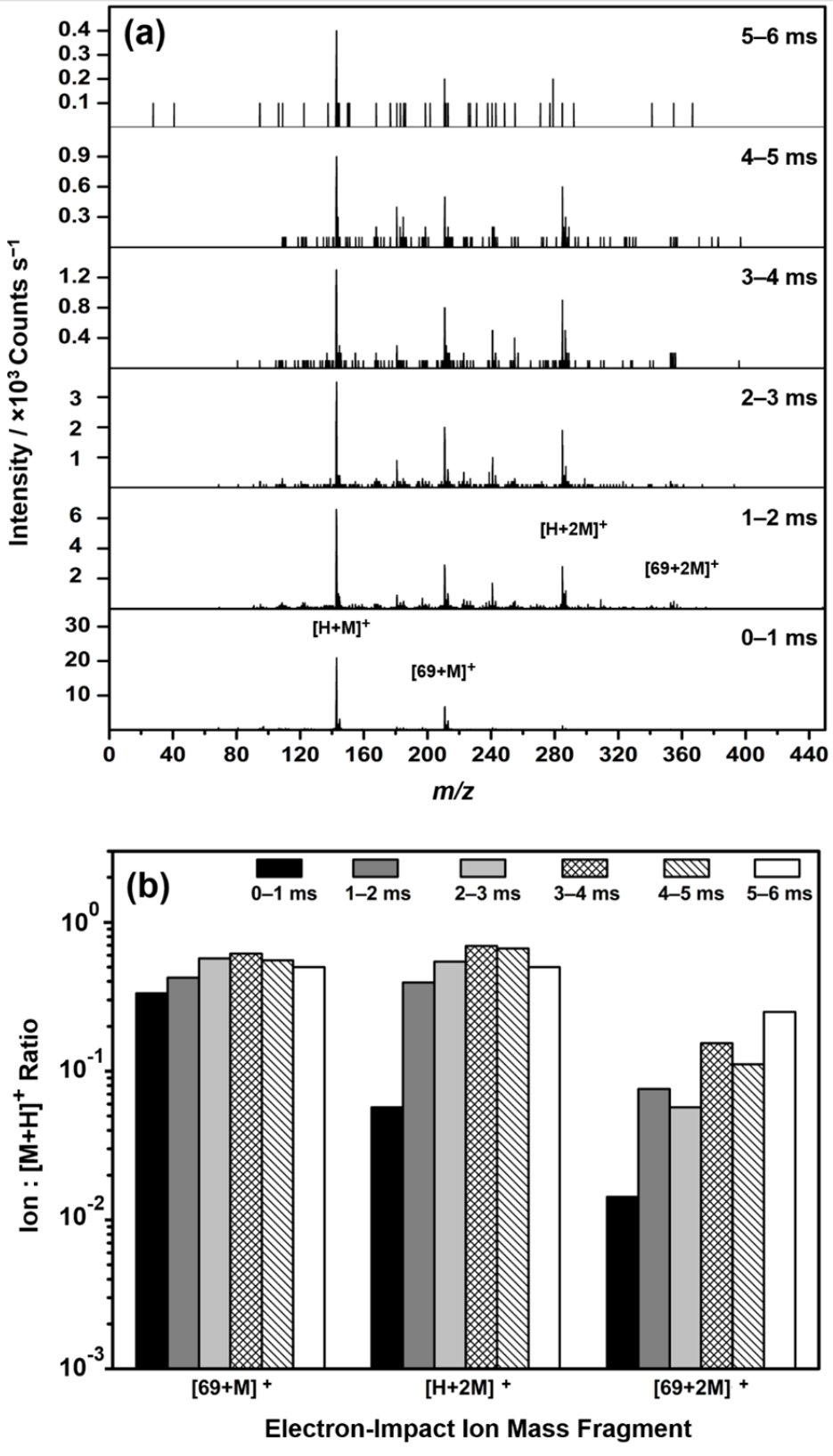

Figure 9: (a) Off-period 20 eV electron-impact ionisation mass spectra taken during consecutive 1 ms sampling time windows for glycidyl methacrylate pulsed plasma (t_{on} = 30 µs, ms t_{off} = 10 ms, P_{on} = 15 W, and 0.1 mbar pressure); and (b) variation of mass fragments between consecutive 1 ms sampling time windows during the off-period, showing relative fragment : protonated molecular ion (143 *m/z*) intensity ratios. Mass spectrometer tuning optimised on 211 *m/z* mass signal.

DISCUSSION

The high levels of plasmachemical reaction pathway selectivity observed by mass spectrometry for the pulsed electrical discharge of glycidyl methacrylate precursor complements the earlier reported time-of-flight secondary ion mass spectrometry (ToF-SIMS) spectra of pulsed plasma deposited poly(glycidyl methacrylate) nanolayers.[16]

This in situ mass spectrometry provides direct evidence for a highly selective step-wise monomer addition polymerisation mechanism occurring during pulsed plasma excitation which underpins the growth of structurally well-defined poly(glycidyl methacrylate) thin films, Figure 5 and Figure 8. There are two distinct reaction regimes corresponding to the short on-period (t_{on}) and long off-period (t_{off}) time windows, Scheme 1. The former corresponds to electrical discharge ignition occurring on the microsecond (μs) timescale to create two initiator species: methacryolyl (69 *m/z*—which is the main fragment formed following low energy electron impact of glycidyl methacrylate precursor, Figure 3), and the protonated monomer (143 *m/z*).[16,17,54,55] This is followed by conventional polymerisation reactions proceeding during the subsequent longer millisecond (ms) off-period timescale, with monomer units sequentially adding to the growing polymer chain, Scheme 1.[17,24,56,57] Both positive ions and radicals at 69 m/z and 143 m/z act as initiators for the off-period polymerisation reaction pathway, Figure 5 and Figure 8 respectively. This is accompanied by an increase in relative intensity of the higher mass oligomeric species during the off-period, Figure 6 and Figure 9.

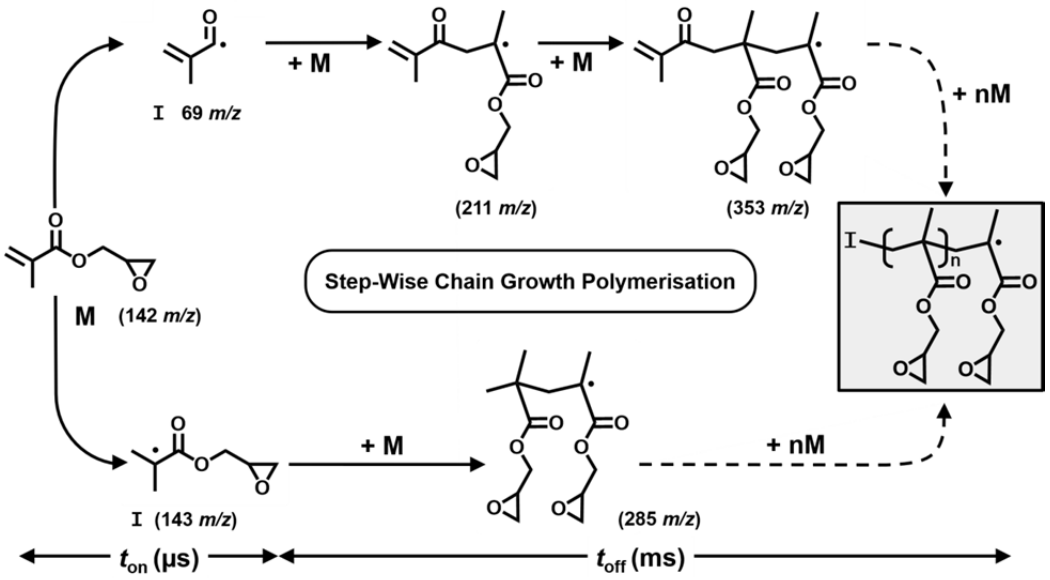

Scheme 1: Free radical chain growth polymerisation mechanism for glycidyl methacrylate pulsed plasma deposition (a similar mechanism could be envisaged for the corresponding 69 *m/z* and 143 *m/z* positive plasma ion initiator species).

The ultra-high reaction pathway selectivities observed in the present investigation are in marked contrast compared to previous time-resolved in situ mass spectrometry studies of pulsed plasmas—where highly selective reaction pathways (product formation) have not been reported for monomers such as: acrylic and methacrylic precursors, styrenic monomers, thiols, amines, silanes, terpenoids, or saturated and unsaturated linear hydrocarbons.[19,20,22,23,25,58,59,60] This can be attributed to the earlier use of longer on-periods (t_{on} = milliseconds), whereas in the present study shorter t_{on} values (in the microsecond range) are employed which narrows the time frame for any damaging cascading plasmachemical fragmentation reaction pathways as well as prohibiting the build-up of the plasma sheath potential leading to ion bombardment damage.[61] Growth of well-defined oligomer species is achieved as a consequence of selecting short micro-millisecond pulsed plasma duty cycles and low powers. This is accompanied by the formation of high mass ions via plasma electron-impact ionisation of high mass radicals within the electrical discharge—which accounts for the absence of any significant difference in mass fragments between positive ion versus low energy electron-impact detection modes, Figure 4 and Figure 7.[62,63] The degree of ionisation in such glow discharge plasmas is very low (10^{-4}–10^{-6}), and hence neutral species are present in much higher concentrations.[64,65] Furthermore, the duration of each plasma pulse is very short (t_{on} = microseconds) relative to the extinction period (t_{off} = milliseconds), hence the

concentration of ions is further diluted. On this basis, a cationic polymerisation mechanism is not expected to be predominant.[66]

CONCLUSIONS

High selectivity reaction pathways for low duty cycle pulsed electrical discharges have been identified using in situ time-resolved mass spectrometry. For glycidyl methacrylate precursor, short electrical discharge pulses (t_{on} = microseconds timescale) lead to the creation of initiator species (the main low energy electron-impact fragment of glycidyl methacrylate (69 *m/z*)) and hydrogen atom addition to the molecular precursor (143 *m/z*). These initiator species then undergo sequential monomer addition within the extended off-period window (t_{off} = milliseconds timescale) giving rise to the growth of well-defined epoxide-functionalised polymer chains. These plasmachemical mechanisms should be applicable to other precursors employed for the low duty cycle pulsed plasma deposition of functional nanolayers.

FUNDING

A. C. thanks P2i Ltd. for a PhD studentship.

ACKNOWLEDGEMENTS

We thank Dr. C. Greenwood and S. Bort at Hiden Analytical Ltd. for technical support.

AUTHOR CONTRIBUTIONS

J. P. S. B. and A. C. devised the experiments. A. C. performed the experiments. The manuscript was jointly drafted by J. P. S. B. and A. C. Both authors gave final approval for publication.

DATA ACCESS

Data created during this research can be accessed at:
https://collections.durham.ac.uk

REFERENCES

1 Gross, E.; Liu, J. H.-C.; Toste, F. D.; Somorjai, G. A. Control of Selectivity in Heterogeneous Catalysis by Tuning Nanoparticle Properties and Reactor Residence Time. *Nat. Chem.* **2012**, *4*, 947–952.

2 Kyriakou, G.; Boucher, M. B.; Jewell, A. D.; Lewis, E. a; Lawton, T. J.; Baber, A. E.; Tierney, H. L.; Flytzani-Stephanopoulos, M.; Sykes, E. C. H. Isolated Metal Atom Geometries as a Strategy for Selective Heterogeneous Hydrogenations. *Science* **2012**, *335*, 1209–1212.

3 Jakuttis, M.; Schönweiz, A.; Werner, S.; Franke, R.; Wiese, K. D.; Haumann, M.; Wasserscheid, P. Rhodium-Phosphite SILP Catalysis for the Highly Selective Hydroformylation of Mixed C4 Feedstocks. *Angew. Chemie - Int. Ed.* **2011**, *50*, 4492–4495.

4 Pindur, U.; Lutz, G.; Otto, C. Acceleration and Selectivity Enhancement of Diels-Alder Reactions by Special and Catalytic Methods. *Chem. Rev.* **1993**, *93*, 741–761.

5 Witte, P. T.; Boland, S.; Kirby, F.; van Maanen, R.; Bleeker, B. F.; de Winter, D. A. M.; Post, J. A.; Geus, J. W.; Berben, P. H. NanoSelect Pd Catalysts: What Causes the High Selectivity of These Supported Colloidal Catalysts in Alkyne Semi-Hydrogenation? *ChemCatChem* **2013**, *5*, 582–587.

6 Jenner, G. High Pressure and Selectivity in Organic Reactions. *Tetrahedron* **1997**, *53*, 2669–2695.

7 Bourne, J. R. Mixing and the Selectivity of Chemical Reactions. *Org. Process Res. Dev.* **2003**, *7*, 471–508.

8 Mellmer, M. A.; Sener, C.; Gallo, J. M. R.; Luterbacher, J. S.; Alonso, D. M.; Dumesic, J. A. Solvent Effects in Acid-Catalyzed Biomass Conversion Reactions. *Angew. Chemie Int. Ed.* **2014**, *53*, 11872–11875.

9 Mushrif, S. H.; Caratzoulas, S.; Vlachos, D. G. Understanding Solvent Effects in the Selective Conversion of Fructose to 5-Hydroxymethyl-Furfural: A Molecular Dynamics Investigation. *Phys. Chem. Chem. Phys.* **2012**, *14*, 2637.

10 Schwartz, T. J.; Bond, J. Q. A Thermodynamic and Kinetic Analysis of Solvent-Enhanced Selectivity in Monophasic and Biphasic Reactor Systems. *Chem. Commun.* **2017**, *53*, 8148–8151.

11 Bayer, T.; Himmler, K. Mixing and Organic Chemistry. *Chem. Eng. Technol.* **2005**, *28*, 285–289.

12 Friedrich, J. Mechanisms of Plasma Polymerization - Reviewed from a Chemical Point of View. *Plasma Process. Polym.* **2011**, *8*, 783–802.

13 Ryan, M. E.; Hynes, A. M.; Badyal, J. P. S. Pulsed Plasma Polymerization of Maleic Anhydride. *Chem. Mater.* **1996**, 8, 37–42.

14 Savage, C. R.; Timmons, R. B.; Lin, J. W. Molecular Control of Surface Film Compositions via Pulsed Radio-Frequency Plasma Deposition of Perfluoropropylene Oxide. *Chem. Mater.* **1991**, *3*, 575–577.

15 Badyal, J. P. S.; Coulson, S. R.; Willis, C.; Brewer, S. A. Surface Coatings. Patent US6551950B1, April 22, 2003.

16 Tarducci, C.; Kinmond, E. J.; Badyal, J. P. S.; Brewer, S. A.; Willis, C. Epoxide-Functionalized Solid Surfaces. *Chem. Mater.* **2000**, *12*, 1884–1889.

17 Boscher, N. D.; Hilt, F.; Duday, D.; Frache, G.; Fouquet, T.; Choquet, P. Atmospheric Pressure Plasma Initiated Chemical Vapor Deposition Using Ultra-Short Square Pulse Dielectric Barrier Discharge. *Plasma Process. Polym.* **2015**, *12*, 66–74.

18 Kinmond, E. J.; Coulson, S. R.; Badyal, J. P. S.; Brewer, S. A.; Willis, C. High Structural Retention during Pulsed Plasma Polymerization of 1H,1H,2H-Perfluorododecene: An NMR and TOF-SIMS Study. *Polymer* **2005**, *46*, 6829–6835.

19 Haddow, D.; France, R.; Short, R. A Mass Spectrometric and Ion Energy Study of the Continuous Wave Plasma Polymerization of Acrylic Acid. *Langmuir* **2000**, *12*, 5654–5660.

20 Fraser, S.; Short, R. D.; Barton, D.; Bradley, J. W. A Multi-Technique Investigation of the Pulsed Plasma and Plasma Polymers of Acrylic Acid: Millisecond Pulse Regime. *J. Phys. Chem. B* **2002**, *106*, 5596–5603.

21 O'Toole, L.; Beck, A. J.; Ameen, A. P.; Jones, F. R.; Short, R. D. Radiofrequency-Induced Plasma Polymerisation of Propenoic Acid and Propanoic Acid. *J. Chem. Soc. Faraday Trans.* **1995**, *91*, 3907.

22 O'Toole, L.; Short, R. D.; Ameen, A. P.; Jones, F. R. Mass Spectrometry of and Deposition-Rate Measurements from Radiofrequency-Induced Plasmas of Methyl Isoburate, Methyl Methacrylate and N-Butyl Methacrylate. *J. Chem. Soc. Faraday Trans.* **1995**, *91*, 1363–1370.

23 Ahmad, J.; Bazaka, K.; Whittle, J. D.; Michelmore, A.; Jacob, M. V. Structural Characterization of γ-Terpinene Thin Films Using Mass Spectroscopy and X-Ray Photoelectron Spectroscopy. *Plasma Process. Polym.* **2015**, *12*, 1085–1094.

24 Swindells, I.; Voronin, S. A.; Bryant, P. M.; Alexander, M. R.; Bradley, J. W. Temporal Evolution of an Electron-Free Afterglow in the Pulsed Plasma Polymerisation of Acrylic Acid. *J. Phys. Chem. B* **2008**, *112*, 3938–3947.

25 Deschenaux, C.; Affolter, A.; Magni, D.; Hollenstein, C.; Fayet, P. Investigations of CH_4, C_2H_2 and C_2H_4 Dusty RF Plasmas by Means of FTIR Absorption Spectroscopy and Mass Spectrometry. *J. Phys. D. Appl. Phys.* 1999, *32*, 1876–1886.

26 Coulson, S. R.; Woodward, I. S.; Badyal, J. P. S.; Brewer, S. A.; Willis, C. Ultralow Surface Energy Plasma Polymer Films. *Chem. Mater.* **2000**, *12*, 2031–2038.

27 Oehr, C.; Müller, M.; Elkin, B.; Hegemann, D.; Vohrer, U. Plasma Grafting — A Method to Obtain Monofunctional Surfaces. *Surf. Coatings Technol.* **1999**, *116–119*, 23–25.

28 Schofield, W. C. E.; McGettrick, J. D.; Badyal, J. P. S. A Substrate-Independent Approach for Cyclodextrin Functionalized Surfaces. *J. Phys. Chem. B* **2006**, *110*, 17161–17166.

29 Harris, L. G.; Schofield, W. C. E.; Badyal, J. P. S. MultiFunctional Molecular Scratchcards. *Chem. Mater.* **2007**, *19*, 1546–1551.

30 Thierry, B.; Jasieniak, M.; de Smet, L. C. P. M.; Vasilev, K.; Griesser, H. J. Reactive Epoxy-Functionalized Thin Films by a Pulsed Plasma Polymerization Process. *Langmuir* **2008**, *24*, 10187–10195.

31 Coad, B. R.; Jasieniak, M.; Griesser, S. S.; Griesser, H. J. Controlled Covalent Surface Immobilisation of Proteins and Peptides Using Plasma Methods. *Surf. Coatings Technol.* **2013**, *233*, 169–177.

32 Yang, G. H.; Kang, E. T.; Neoh, K. G. Surface Modification of Poly(tetrafluoroethylene) Films by Plasma Polymerization of Glycidyl Methacrylate and Its Relevance to the Electroless Deposition of Copper. *J. Polym. Sci. Part A Polym. Chem.* **2000**, *38*, 3498–3509.

33 Camporeale, G.; Moreno-Couranjou, M.; Bonot, S.; Mauchauffé, R.; Boscher, N. D.; Bebrone, C.; Van de Weerdt, C.; Cauchie, H.-M.; Favia, P.; Choquet, P. Atmospheric-Pressure Plasma Deposited Epoxy-Rich Thin Films as Platforms for Biomolecule Immobilization-Application for Anti-Biofouling and Xenobiotic-Degrading Surfaces. *Plasma Process. Polym.* **2015**, *12*, 1208–1219.

34 Bonot, S.; Mauchauffé, R.; Boscher, N. D.; Moreno-Couranjou, M.; Cauchie, H.; Choquet, P. Self-Defensive Coating for Antibiotics Degradation—Atmospheric Pressure Chemical Vapor Deposition of Functional and Conformal Coatings for the Immobilization of Enzymes. *Adv. Mater. Interfaces,* **2015**, 2, 1500253.

35 Brown, P. S.; Wood, T. J.; Schofield, W. C. E.; Badyal, J. P. S. A Substrate-Independent Lift-Off Approach for Patterning Functional Surfaces. *ACS Appl. Mater. Interfaces* **2011**, *3*, 1204–1209

36 Carletto, A.; Badyal, J. P. S. Mechanistic Reaction Pathway for Hexafluoropropylene Oxide Pulsed Plasma Deposition of PTFE-like Films. *J. Phys. Commun.* **2017**, *1*, 55024.

37 Bradley, J. W.; Bryant, P. M. The Diagnosis of Plasmas Used in the Processing of Textiles and Other Materials. In Plasma Technologies for Textiles; Elsevier, 2007; pp 25–63.

38 Steiner, R. E.; Lewis, C. L.; King, F. L. Time-of-Flight Mass Spectrometry with a Pulsed Glow Discharge Ionization Source. *Anal. Chem.* **1997**, *69*, 1715–1721.

39 Lewis, C. L.; Moser, M. A.; Dale, D. E.; Hang, W.; Hassell, C.; King, F. L.; Majidi, V. Time-Gated Pulsed Glow Discharge: Real-Time Chemical Speciation at the Elemental,

Structural, and Molecular Level for Gas Chromatography Time-of-Flight Mass Spectrometry. *Anal. Chem.* **2003**, *75*, 1983–1996.

40 Li, L.; Millay, J. T.; Turner, J. P.; King, F. L. Millisecond Pulsed Radio Frequency Glow Discharge Time of Flight Mass Spectrometry: Temporal and Spatial Variations in Molecular Energetics. *J. Am. Soc. Mass Spectrom.* **2004**, *15*, 87–102.

41 Kawamura, E.; Vahedi, V.; Lieberman, M. A.; Birdsall, C. K. Ion Energy Distributions in Rf Sheaths; Review, Analysis and Simulation. *Plasma Sources Sci. Technol.* **1999**, *8*, R45–R64.

42 Voronin, S. A; Alexander, M. R.; Bradley, J. W. Time-Resolved Measurements of the Ion Energy Distribution Function in a Pulsed Discharge Using a Double Gating Technique. *Meas. Sci. Technol.* **2005**, *16*, 2446–2452.

43 Voronin, S. A.; Alexander, M. R.; Bradley, J. W. Time-Resolved Mass and Energy Spectral Investigation of a Pulsed Polymerising Plasma Struck in Acrylic Acid. *Surf. Coatings Technol.* **2006**, *201*, 768–775.

44 Voronin, S. a; Zelzer, M.; Fotea, C.; Alexander, M. R.; Bradley, J. W. Pulsed and Continuous Wave Acrylic Acid Radio Frequency Plasma Deposits: Plasma and Surface Chemistry. *J. Phys. Chem. B* **2007**, *111*, 3419–3429.

45 Mishra, A.; Clarke, G.; Kelly, P.; Bradley, J. W. High Temporal Resolution Ion Energy Distribution Functions in HIPIMS Discharges. *Plasma Process. Polym.* **2009**, *6*, S610–S614.

46 EQP and EQS Analysers Hiden Analytical Technical Information, https://www.hiden.de/wpcontent/uploads/pdf/EQP_and_EQS__Hiden_Analytical_Technical_Inofrmation.pdf (Accessed: 15 January 2018).

47 Bohlmark, J.; Lattemann, M.; Gudmundsson, J. T.; Ehiasarian, A. P.; Aranda Gonzalvo, Y.; Brenning, N.; Helmersson, U. The Ion Energy Distributions and Ion Flux Composition from a High Power Impulse Magnetron Sputtering Discharge. *Thin Solid Films* **2006**, *515*, 1522–1526.

48 Hecimovic, A.; Ehiasarian, A. P. Time Evolution of Ion Energies in HIPIMS of Chromium Plasma Discharge. J*. Phys. D. Appl. Phys.* **2009**, *42*, 135209.

49 Zimmerman, P. A.; Hercules, D. M.; Benninghoven, A. Time-of-Flight Secondary Ion Mass Spectrometry of Poly(alkyl Methacrylates). *Anal. Chem.* **1993**, *65*, 983–991.

50 Eccles, A. J.; Vickerman, J. C. The Characterization of an Imaging Time-of-flight Secondary Ion Mass Spectrometry Instrument. *J. Vac. Sci. Technol. A Vacuum, Surfaces, Film.* **1989**, *7*, 234–244.

51 Brown, R. M.; Creaser, C. S. The Electron Impact and Chemical Ionization Mass Spectra of Some Glycidyl Ethers. *Org. Mass Spectrom.* **1980**, *15*, 578–581.

52 Yildirim, Y.; Balcan, M.; Bass, A. D.; Cloutier, P.; Sanche, L. Electron Stimulated Desorption of Anions and Cations from Condensed Allyl Glycidyl Ether. *Phys. Chem. Chem. Phys.* **2010**, *12*, 7950–7958.

53 NIST National Institute of Standard and Technology, US Department of Commerce http://webbook.nist.gov/cgi/cbook.cgi?ID=C106912&Mask=200#Mass-Spec (Accessed: 5 Feb 2018).

54 Ryan, M. E.; Hynes, A. M.; Badyal, J. P. S. Pulsed Plasma Polymerization of Maleic Anhydride. *Chem. Mater.* **1996**, *8*, 37–42.

55 Mishra, G.; McArthur, S. L. Plasma Polymerization of Maleic Anhydride: Just What Are the Right Deposition Conditions? *Langmuir* **2010**, *26*, 9645–9658.

56 Manakhov, A.; Moreno-Couranjou, M.; Boscher, N. D.; Rogé, V.; Choquet, P.; Pireaux, J. J. Atmospheric Pressure Pulsed Plasma Copolymerisation of Maleic Anhydride and Vinyltrimethoxysilane: Influence of Electrical Parameters on Chemistry, Morphology and Deposition Rate of the Coatings. *Plasma Process. Polym.* **2012**, *9*, 435–445.

57 Klages, C.-P.; Höpfner, K.; Kläke, N.; Thyen, R. Surface Functionalization at Atmospheric Pressure by DBD-Based Pulsed Plasma Polymerization. *Plasmas Polym.* **2000**, *5*, 79–89

58 Beck, A. J.; Jones, F. R.; Short, R. D. Mass Spectrometric Study of the Radiofrequency-Induced Plasma Polymerisation of Styrene and Propenoic Acid. *J. Chem. Soc. Faraday Trans.* **1998**, *94*, 559–565.

59 Thiry, D.; Britun, N.; Konstantinidis, S.; Dauchot, J.-P. J.-P.; Guillaume, M.; Cornil, J.; Snyders, R. Experimental and Theoretical Study of the Effect of the Inductive-to-

Capacitive Transition in Propanethiol Plasma Polymer Chemistry. *J. Phys. Chem. C* **2013**, *117*, 9843–9851.

60 Michelmore, A.; Bryant, P. M.; Steele, D. A.; Vasilev, K.; Bradley, J. W.; Short, R. D. Role of Positive Ions in Determining the Deposition Rate and Film Chemistry of Continuous Wave Hexamethyl Disiloxane Plasmas. *Langmuir* **2011**, *27*, 11943–11950.

61 Mackie, N. M.; Dalleska, N. F.; Castner, D. G.; Fisher, E. R. Comparison of Pulsed and Continuous-Wave Deposition of Thin Films from Saturated Fluorocarbon/H_2 Inductively Coupled Rf Plasmas. *Chem. Mater.* **1997**, 9, 349–362.

62 Kushner, M. J. A Model for the Discharge Kinetics and Plasma Chemistry during Plasma Enhanced Chemical Vapor Deposition of Amorphous Silicon. *J. Appl. Phys.* **1988**, 63, 2532–2551.

63 Schwarzenbach, W.; Cunge, G.; Booth, J. P. High Mass Positive Ions and Molecules in Capacitively-Coupled Radio-Frequency CF_4 Plasmas. *J. Appl. Phys.* **1999**, 85, 7562.

64 Plasma Surface Modification and Plasma Chemistry Schram. D. C.; Bisschops, Th. H. J.; Kroesen, G. M. W.; de Hoog, F. J.; *Plasma Phys. Control. Fusion* **1987**, *29*, 1353–1364.

65 Grill, A. Cold Plasma in Materials Fabrication: From Fundamentals to Applications, IEEE Press: Piscataway, NJ, 1994, p7.

66 Saboohi, S.; Coad, B.; Griesser, H.; Michelmore, A.; Short, R. Synthesis of Highly Functionalised Plasma Polymer Films from Protonated Precursor Ions via the Plasma α–γ Transition. *Physical Chemistry Chemical Physics* **2017**, 19, 5637–5646.